

Fast calcium wave propagation mediated by electrically conducted excitation and boosted by CICR

J. M. A. M. Kusters, W. P. M. van Meerwijk, D. L. Ypey, A. P. R. Theuvsenet and C. C. A. M. Gielen

Am J Physiol Cell Physiol 294:917-930, 2008. First published Jan 16, 2008;
doi:10.1152/ajpcell.00181.2007

You might find this additional information useful...

This article cites 46 articles, 25 of which you can access free at:

<http://ajpcell.physiology.org/cgi/content/full/294/4/C917#BIBL>

Updated information and services including high-resolution figures, can be found at:

<http://ajpcell.physiology.org/cgi/content/full/294/4/C917>

Additional material and information about *AJP - Cell Physiology* can be found at:

<http://www.the-aps.org/publications/ajpcell>

This information is current as of July 30, 2008 .

Fast calcium wave propagation mediated by electrically conducted excitation and boosted by CICR

J. M. A. M. Kusters,¹ W. P. M. van Meerwijk,² D. L. Ypey,² A. P. R. Theuvenet,² and C. C. A. M. Gielen¹

¹Department of Biophysics and ²Department of Cell Biology, Radboud University Nijmegen, Nijmegen, The Netherlands

Submitted 2 May 2007; accepted in final form 13 January 2008

Kusters JM, van Meerwijk WP, Ypey DL, Theuvenet AP, Gielen CC. Fast calcium wave propagation mediated by electrically conducted excitation and boosted by CICR. *Am J Physiol Cell Physiol* 294: C917–C930, 2008. First published January 16, 2008; doi:10.1152/ajpcell.00181.2007.—We have investigated synchronization and propagation of calcium oscillations, mediated by gap junctional excitation transmission. For that purpose we used an experimentally based model of normal rat kidney (NRK) cells, electrically coupled in a one-dimensional configuration (linear strand). Fibroblasts such as NRK cells can form an excitable syncytium and generate spontaneous inositol 1,4,5-trisphosphate (IP₃)-mediated intracellular calcium waves, which may spread over a monolayer culture in a coordinated fashion. An intracellular calcium oscillation in a pacemaker cell causes a membrane depolarization from within that cell via calcium-activated chloride channels, leading to an L-type calcium channel-based action potential (AP) in that cell. This AP is then transmitted to the electrically connected neighbor cell, and the calcium inflow during that transmitted AP triggers a calcium wave in that neighbor cell by opening of IP₃ receptor channels, causing calcium-induced calcium release (CICR). In this way the calcium wave of the pacemaker cell is rapidly propagated by the electrically transmitted AP. Propagation of APs in a strand of cells depends on the number of terminal pacemaker cells, the L-type calcium conductance of the cells, and the electrical coupling between the cells. Our results show that the coupling between IP₃-mediated calcium oscillations and AP firing provides a robust mechanism for fast propagation of activity across a network of cells, which is representative for many other cell types such as gastrointestinal cells, urethral cells, and pacemaker cells in the heart.

gap junctions; calcium waves; pacemaking; electrical coupling; action potential propagation; inositol 1,4,5-trisphosphate receptor; normal rat kidney cell; calcium-induced calcium release

INTRACELLULAR CALCIUM OSCILLATIONS are very common and have been reported in a large variety of cell types, such as smooth muscle cells (39), hepatocytes (47), oocytes (5), normal rat kidney (NRK) fibroblast cells (16), and pancreatic acinar cells (11, 33). In these cell types, the cytosolic calcium transients are evoked by inositol 1,4,5-trisphosphate (IP₃)-linked agonist stimulation: after interacting with cell-surface receptors, agonists activate phospholipase C and induce the release of IP₃. IP₃ then triggers calcium release from intracellular stores through IP₃-sensitive calcium release channels in the endoplasmic reticulum (ER) membrane (32). Calcium liberation from the ER can also be activated by cytosolic calcium in the presence of IP₃. In our model, the main mechanism of calcium-induced calcium release (CICR) is the opening of the IP₃ receptor (but other release mechanisms of intracellular calcium may do as well).

In the cell types mentioned above, the cells are connected by gap junctions, allowing diffusion of IP₃ and calcium. Since both IP₃ and calcium facilitate intracellular calcium oscillations, diffusion of calcium and IP₃ through the gap junctions could provide an effective way for synchronization of intracellular calcium oscillations in neighboring cells and for propagation of waves of intracellular calcium oscillations through the network (see e.g., Refs. 10, 19, 20, 40). The propagation of calcium waves through the network has been the topic of many studies, but the cellular mechanisms involved in the propagation of calcium oscillations can be very different. Most studies refer to the propagation of calcium waves in nonexcitable cells with intracellular IP₃-mediated calcium oscillations, where oscillations in cells are coupled by diffusion of IP₃ and calcium through gap junctions (see e.g., Refs. 12, 19, 20, 43). In our study, we ignore coupling of oscillations by calcium and IP₃ diffusion for good reasons, which are explained in the DISCUSSION.

On the other hand, there is propagation of electrical activity in networks of cells electrically coupled by gap junctions, such as in the ventricular myocardium (17, 18, 23–26). In such types of cell networks, propagation of electrical activity is the result of depolarization of a cell by action potential (AP) firing of its neighbor. For adequate gap junctional coupling, an AP causes a depolarization in neighboring cells, which opens their membrane channels and so triggers an AP.

Some recent studies have focused on cell types that have both IP₃-mediated calcium oscillations and APs, such as in interstitial cells of Cajal (ICC) (4), sinoatrial nodal cells in the heart (31), lymphatic smooth muscle cells (22), and NRK fibroblasts (27). These cell types have the interesting property that the mechanisms of IP₃-mediated calcium oscillation and AP generation are coupled and interact with each other (28). An AP can trigger a calcium transient, since inflow of calcium during an AP causes CICR. In the other direction, the increase of cytosolic calcium due to release of calcium through the IP₃ receptor opens calcium-dependent channels in the membrane, causing a depolarization. In NRK cells, the major calcium-dependent membrane channel type is the calcium-dependent chloride channel (Cl_{Ca}) with a Nernst potential near –20 mV. This depolarization may then trigger an AP (6, 27). Since electrical coupling through gap junctions is faster than chemical coupling by diffusion of calcium and IP₃ through gap junctions (6, 36), the intracellular calcium oscillations between cells are also (indirectly) coupled by the electrical coupling by gap junctions.

Because of the positive interaction between the IP₃-mediated calcium oscillator and membrane depolarization, excitable

Address for reprint requests and other correspondence: C. C. A. M. Gielen, Dept. of Biophysics, Radboud Univ. Nijmegen, Geert Grooteplein 21, 6525 EZ Nijmegen, The Netherlands (e-mail: s.gielen@science.ru.nl).

The costs of publication of this article were defrayed in part by the payment of page charges. The article must therefore be hereby marked “advertisement” in accordance with 18 U.S.C. Section 1734 solely to indicate this fact.

cells with IP₃-mediated calcium oscillations may be very robust pacemakers for propagating activity in the network (45). Recently, Imtiaz et al. (22) investigated the various coupling modes of two cells with different amounts of IP₃ and, therefore, different intrinsic oscillation frequencies. These authors showed that the chemical and electrical coupling by gap junctions can cause anti-phase or in-phase oscillations of the cell pair, depending on the amount of IP₃. Moreover, these authors showed that weak coupling (small conductance of the gap junction) is sufficient to synchronize heterogeneous cell pairs.

Following up on the study by Imtiaz et al. (22) on a pair of cells, we have investigated the initiation and propagation of activity in a network with excitable cells with IP₃-mediated calcium oscillators by gap junctional coupling. Imtiaz et al. (22) showed that a pacemaker cell can drive the calcium oscillations in a neighboring cell with a lower IP₃ concentration and a correspondingly lower intrinsic oscillation frequency. The questions that we have addressed are, What happens when more cells with a low IP₃ concentration are coupled to this single pacemaker? And what happens if a pacemaker is coupled to cells that do not have an intrinsic oscillation frequency, because the IP₃ concentration is too small? If that number of coupled follower cells increases, the current from the pacemaker cell to the follower cells will spread through the whole network. When the gap junctional conductance is very small, the current might be too small to depolarize the neighboring cells. However, when the gap junctional conductance is very large, current will spread throughout the network, and if the network is large, the net current into a neighboring cell may also be too small to depolarize the cell. Therefore, in agreement with previous studies on excitable cells without intracellular calcium oscillations (36), we expect an optimal range of gap junctional conductances for initiation and propagation of activity in the network. Because of the positive, reinforcing coupling between the intracellular calcium oscillator and the membrane depolarization, we hypothesize that propagation is more robust in excitable cells with both mechanisms compared with that in cells that lack one of the two.

We address these problems using an experimentally verified model for NRK fibroblast cells (27). Contrary to Imtiaz et al. (22), we did not include voltage-dependent IP₃ synthesis. The coupling between cells in our study is by electrical current through the gap junctions. In each individual cell, the electrical phenomena are coupled to the intracellular calcium oscillators by the calcium inflow through the L-type calcium channels and by calcium inflow through the IP₃ receptor. In the DISCUSSION we evaluate the consequences of this simplification on the propagation of activity.

METHODS

Model Description

In previous studies, we have reported a mathematical model of NRK fibroblasts capturing the basic characteristics (27, 28) based on single-cell data (14). This model was obtained by implementation of the dynamics of the membrane ion channels and the intracellular calcium oscillator. As an emergent property, the model correctly reproduces the properties of calcium transients, calcium APs, and the coupling between calcium transients and calcium APs.

The model contains two compartments for each cell: the cytosol and the ER. The plasma membrane contains a plasma membrane

calcium-ATPase (PMCA) pump, L-type calcium channels, Cl_{Ca} channels, a nonspecific leak, and inward rectifying potassium channels (14). The ER membrane contains a sarco(endo)plasmic reticulum calcium-ATPase (SERCA) pump, a calcium leak, and an IP₃ receptor channel. Cells are electrically coupled by gap junctions.

The key idea of the model (27) is that autocrine and paracrine production of hormones such as PGF_{2α} leads to the production of IP₃, which gives rise to IP₃-mediated intracellular calcium oscillations. These IP₃-mediated calcium oscillations cause periodic calcium transients, which open the Cl_{Ca} channels. These Cl_{Ca} channels depolarize the membrane toward the chloride Nernst potential, near -20 mV, thereby causing activation of the L-type calcium channels. Opening of calcium channels generates an influx of calcium in the cells with a concomitant further depolarization toward the equilibrium potential for calcium ions. The Cl_{Ca} channels remain activated as long as the intracellular calcium level is elevated, resulting in a plateau phase at the chloride Nernst potential at -20 mV. Upon extrusion of calcium from the cytoplasm, the Cl_{Ca} channels become deactivated, and the cells subsequently repolarize to -70 mV as a result of the activity of inward rectifier potassium channels (14). Just the other way around, calcium APs induce CICR through the IP₃ receptors.

The autonomous cell oscillator. The NRK cell model by Kusters et al. (27) that describes the dynamics of the cell has two major components: an IP₃-mediated intracellular calcium oscillator and an electrically excitable membrane. In this report we describe the main properties of the NRK cell. For more details, we refer to Ref. 27.

Calcium in the cytosol plays a key role in coupling the dynamics of the IP₃-mediated calcium oscillator and the cell membrane (28). The rate of change in the membrane potential due to the currents through inward rectifier potassium channels (I_{Kir}), L-type calcium channels (I_{CaL}), Cl_{Ca} channels [$I_{Cl(Ca)}$], leak channels (I_{leak}), and store-dependent calcium (SDC) channels (I_{SDC}) is given by Eq. A1 in the APPENDIX, where I_{Kir} and I_{leak} determine the membrane potential of the cell at rest near -70 mV and are specified by Eqs. A2–A6.

In NRK cells, the crucial coupling between electrical events at the excitable membrane and the internal calcium oscillations is controlled by the L-type calcium channel and the Cl_{Ca} channel. The current through the L-type calcium channels is given by Eq. A7, where V_m refers to the membrane potential and E_{CaL} refers to the Nernst potential of calcium, near 50 mV. The L-type calcium channel has an activation (m) and an inactivation (h) variable. The dynamics of m and h obey a first-order differential equation with steady-state values m_∞ and h_∞ given by Eqs. A8 and A10, respectively, and with time constants given by Eqs. A9 and A11, respectively.

The current through the Cl_{Ca} channel is given by Eq. A12. In addition, the cell membrane has a SDC channel. The conductance of the SDC is inversely related to the calcium concentration in the ER, as given by Eq. A13.

One of the mechanisms for calcium extrusion from the cytosol is the PMCA pump. The flux of calcium ions through the PMCA pump (J_{PMCA}) is described by Eq. A16.

Any changes in the cytosolic calcium concentration ($[Ca^{2+}]_{cyt}$) are due to buffering of calcium (Eq. A14), to a net flux of calcium through the plasma membrane (J_{PM} ; Eq. A15), and to net fluxes through the ER membrane (Eq. A18). The latter has a constant leak of calcium (J_{leakER} ; Eq. A19), a flux through the IP₃ receptor (J_{IP3R} ; Eq. A20), and active transport of calcium into the ER by the SERCA pump (J_{SERCA} ; Eq. A24).

The intracellular calcium oscillator is controlled by the intracellular IP₃ concentration, which activates the IP₃ receptor. The flux of calcium ions through the IP₃ channel is described by a Hodgkin-Huxley type formalism (Eq. A20) with activation variable f and inactivation variable w , with the steady-state values f_∞ and w_∞ given by Eqs. A21 and A22. The time constant for the activation parameter f is considered to be small relative to that of the other processes in the cell. Therefore, we have used f_∞ instead of f . The time constant τ_w for the inactivation gate is described by Eq. A23. This results in periodic

oscillations of calcium flow out of the ER into the cytosol and calcium reuptake in the ER by activity of the SERCA pump. As suggested by Dupont and Goldbeter (8), the flux of calcium ions through the SERCA pump is described by Eq. A24.

The elevated calcium concentration in the cytosol by opening of the IP₃ receptor activates the Cl_{Ca} channels (see Eq. A12), which depolarize the cell membrane to the chloride Nernst potential, near -20 mV. As explained by Kusters et al. (27), this depolarization can open the L-type calcium channels. Opening of the L-type calcium channels gives rise to a further increase in [Ca²⁺]_{cyt}. As a result, an AP with a plateau phase near -20 mV occurs. Calcium in the cytosol is reduced by reuptake of calcium in the ER by the SERCA and PMCA pumps. When [Ca²⁺]_{cyt} has been restored to its basal level, the Cl_{Ca} channels close and the membrane potential repolarizes to the rest potential, near -70 mV.

Parameter modification. The full set of equations describing the dynamics and the parameter values of this NRK model can be found in Kusters et al. (27). In the present model study, we have had to adjust some parameter values. When calcium in the external medium of NRK cells is replaced by strontium, AP propagation in experiments is more robust (6). The reason is that strontium does not inactivate the L-type calcium channels as calcium does (14). Since many experimental data were obtained using strontium instead of calcium (6, 7, 14), we have omitted the calcium-dependent inactivation factor (v_{Ca}) in the model equation for the L-type calcium channel. Another effect is that the current through the L-type calcium channel is much larger for strontium than for calcium, which is why we have used a larger value for the L-type calcium channel conductance (G_{CaL} : 1.6 nS instead of 0.7 nS). Since the L-type calcium channel, Cl_{Ca} channel, and IP₃ receptor are important channels for AP propagation, and since activation of these channels was rather small in our old model (27), we have changed the following parameters: the time constant for inactivation of the L-type calcium channel (τ_h) is a factor 2 longer, the time constant for activation of the L-type calcium channel (τ_m) is a factor 2 smaller, the membrane potential for half-maximal activation of m_∞ is set to -10 mV, $K_{Cl(Ca)}$ (the half-maximal activation concentration) is set to 18 μ M, J_{PMCA} is set to 3×10^{-5} μ mol/(s·dm²), and leak conductance (G_{leak}) is set to 0.058 nS. These changes lie within the range of values from experimental observations. The k_{on} and k_{off} parameters of the buffer are set to 1. Table 1 shows the modified parameter values.

Electrical coupling through gap junctions. Many fibroblastic cell types in culture, including NRK cells, are electrically coupled by gap junctional channels, e.g., composed of connexin43 (Cx43) subunits with a typical conductance between the cell and its surrounding network near 20 nS (13). The monolayer of NRK cells can be approximated by a hexagonal grid (42). Therefore, the total gap junctional conductance of 20 nS for a cell corresponds to a gap junctional conductance (G_g) between two neighboring cells of

20/6, ~3 nS, which is in agreement with other experimental data for gap junction coupling between cells where Cx43 subunits are involved (3, 41).

The electrical current flowing through the gap junctions between cell i and other cells in the network was incorporated by an extra term at the right-hand side of Eq. A1, which resulted in

$$C_m \frac{dV_m}{dt} = - \left(I_{Kir} + I_{leak} + I_{CaL} + I_{Cl(Ca)} + I_{SDC} + \sum_{j \text{ neighbor } i} I_{gap}^{ij} \right) \quad (1)$$

$$I_{gap}^{ij} = G_g (V_m^i - V_m^j) \quad (2)$$

where G_g is the conductance of the gap junction coupling between neighboring cells i and j .

We modeled the AP propagation by electrical coupling of a single pacemaker cell to surrounding follower cells in a one-dimensional strand (cable). Our aim is to understand the electrical load on the single pacemaker cell due to coupling to surrounding cells. Figure 1A shows the equivalent electrical circuit for the passive electrical properties of a one-dimensional strand of follower cells driven by a pacemaker cell (P). Each follower cell is represented by a capacitance C and resistance R_f , and cells are coupled by the gap junctional resistance R_g . This passive model is a good approximation as long as the membrane potential does not reach the threshold for AP firing.

Expanding a network of n follower cells with an additional follower cell (Fig. 1B) gives a relation between Z_n and Z_{n+1} , where Z_n and Z_{n+1} represent the equivalent impedance for an array with n and $n + 1$ follower cells, respectively. This relation is given by

$$Z_{n+1}(\omega) = \frac{Z_{cell}(\omega)(R_g + Z_n(\omega))}{R_g + Z_n(\omega) + Z_{cell}(\omega)} \quad (3)$$

where $Z_{cell}(\omega)$ is the impedance of a follower cell in the frequency domain, given by

$$Z_{cell}(\omega) = \frac{R_f}{1 + \omega^2 \tau_f^2} - i \frac{R_f \omega \tau_f}{1 + \omega^2 \tau_f^2} \quad (4)$$

with capacitance C , resistance R_f , and the characteristic time constant $\tau_f = R_f C$. The equivalent resistance of an infinitely long one-dimensional strand can be calculated by setting $Z_{n+1}(\omega) = Z_n(\omega)$, which gives

$$Z_\infty = \frac{-R_g + \sqrt{R_g^2 + 4Z_{cell}(\omega)R_g}}{2} \quad (5)$$

For an infinitely large strand of cells, the net current to the first follower cell (see Fig. 1C) is given by

$$I_{cell} = V_p \frac{Z_\infty}{Z_\infty Z_{cell} + (Z_\infty + Z_{cell})(R_g + Z_p)}$$

$$= V_p \left[-R_g + \sqrt{R_g^2 + 4Z_{cell}(\omega)R_g} \right]$$

$$\times \left\{ -R_g + \sqrt{R_g^2 + 4Z_{cell}(\omega)R_g} \right\} Z_{cell} \quad (6)$$

$$+ \left[-R_g + \sqrt{R_g^2 + 4Z_{cell}(\omega)R_g} + 2Z_{cell} \right] (R_g + Z_p) \Big\}^{-1}$$

From Eqs. 5 and 6, it is easy to see that I_{cell} becomes zero for infinitely small values of R_g . If R_g becomes infinitely small, Z_∞ becomes zero, and therefore I_{cell} becomes zero. Equation 6 shows that I_{cell} is also zero for large values of R_g ($R_g \uparrow \infty$, $I_{cell} = 0$). The optimal value of R_g is found by solving $\partial I_{cell} / \partial R_g = 0$. For the parameter values in our study, the optimal value for R_g is $\sim 2.0 \times 10^9 \Omega$ ($G_g = 0.5$ nS).

Table 1. Changed parameter values of the single-cell model

Parameter	Value	Units
$K_{Cl(Ca)}$	18	μ M
G_{CaL}	1.6	nS
G_{leak}	0.058	nS
J_{PMCA}^{max}	3.0×10^{-5}	μ mol/(s·dm ²)
k_{on}	1.0	(μ M·s) ⁻¹
k_{off}	1.0	s ⁻¹
Membrane potential for half-maximal activation of m_∞	-10	mV

$K_{Cl(Ca)}$, half-maximal activation concentration; G_{CaL} , L-type calcium channel conductance; G_{leak} , leak conductance; J_{PMCA}^{max} , flux of calcium ions through the plasma membrane Ca²⁺-ATPase (PMCA) pump; k_{on} and k_{off} , buffer parameters of binding and dissociation; m_∞ , steady-state open activation gate.

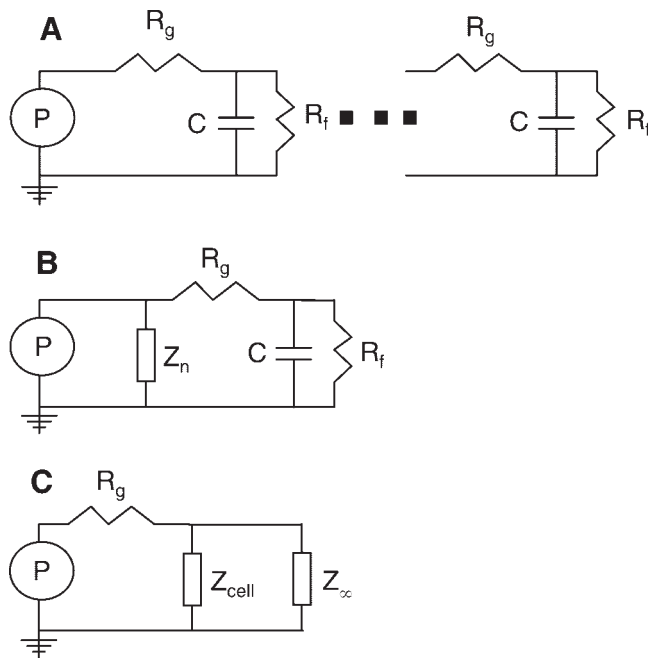


Fig. 1. *A*: electrical circuit for a 1-dimensional network, where a pacemaker cell (P) is coupled by a resistance R_g to n follower cells. Each follower cell is represented by a capacitance C and resistance R_f and is coupled to its neighbors by gap junctions with a resistance R_g . *B*: expansion of a network with n follower cells with an extra follower cell. Z_n , impedance for an array with n follower cells. *C*: schematic circuit of a pacemaker cell coupled to an infinitely large strand of cells with a total impedance Z_∞ . Z_{cell} , impedance of a follower cell.

RESULTS

Phase-Response Curves for Current Pulse and Calcium Pulse

Understanding the response of a single cell to a current pulse or injection of calcium ions is helpful to understand the interaction between two cells (49). Current and calcium perturbations allow us to determine the phase-response curve (PRC), which gives the phase shift ($\Delta\phi$) of the AP or calcium oscillator of a NRK pacemaker cell with intrinsic cycle length (T) as a function of the phase (ϕ) at which the external input is given. When a current pulse of sufficient amplitude is injected into a cell, the elevated membrane potential results in opening of the L-type calcium channels and, possibly, AP firing.

The inflow of calcium causes CICR through the IP_3 receptor channel and gives rise to a phase advance of the IP_3 -mediated calcium oscillator. On the other hand, a calcium injection gives rise to a phase advance of the IP_3 -mediated calcium oscillator and corresponding calcium transient. The resulting depolarization by the Cl_{Ca} channels then leads to advanced appearance of the next AP.

The PRC is measured by delivering a precisely timed perturbation and measuring the change in the running cycle duration. The upstroke of the preceding pacemaker AP is chosen as the reference point (phase zero), since it is very sharp compared with the onset of calcium oscillations. Moreover, calcium oscillations change in shape and size. Phase ϕ is defined by $\phi = t_p/T$, where t_p is the time when the stimulus is applied, relative to the reference point, and the phase change $\Delta\phi$ is defined as $(T - T_{\text{new}})/T$, where T_{new} is the time of

occurrence of the following AP or calcium transient relative to the reference point, i.e., the new cycle length. The PRC quantifies the effect of an input pulse at a given phase on the occurrence of the following AP or calcium transient. If an input pulse does not affect the next AP or calcium transient, T is unchanged and the phase change $\Delta\phi$ at that point of the curve is zero. If the input pulse delays the next AP or calcium transient, $T_{\text{new}} > T$, and the phase change $\Delta\phi$ has a negative value (not observed in our simulations). If the pulse advances the next AP, $T_{\text{new}} < T$, and $\Delta\phi$ is positive. Figure 2 shows PRCs (*bottom panels*) generated by injecting a depolarizing current pulse with a 50-ms duration of 10, 15, and 20 pA (*A*) and a calcium pulse associated with a calcium current injection of 1, 2, and 5 pA for 50 ms (*B*). The *top three subpanels* in Fig. 2 show examples of the effect of current (15 pA in *A*) and calcium pulses (1 pA in *B*) on the phase advance of the AP and calcium oscillation, respectively (dashed lines), and the unperturbed response (solid lines). The *bottom panels* of Fig. 2, *A* and *B*, show the phase change of the IP_3 -mediated calcium oscillator as a function of the timing of the current pulse in the cycle of the calcium oscillator. Figure 2*A*, *bottom*, shows that a current pulse of 10 pA has no effect on the IP_3 -mediated calcium oscillator irrespective of the phase in the AP cycle (thick solid line). Depolarizing current pulses of 15 (dashed-dotted line) and 20 pA (thin solid line) injected at phase $\phi > 0.2$ trigger the next calcium transient almost immediately via an evoked AP. Injection at phase $\phi < 0.1$ has no effect on the next calcium transient, because this period includes the AP and its refractory period (see Fig. 2*A*). Note that these current injections are smaller than the current inflow in the cell by the membrane during an AP, which is ~ 25 pA. Figure 2*B*, *bottom*, shows the phase change of the AP as a function of the phase of the calcium pulse. The phase of the AP does not change for calcium pulses of 1 (thick solid line), 2 (dashed-dotted line), and 5 pA (thin solid line) at phases $\phi < 0.6$, $\phi < 0.4$, and $\phi < 0.3$, respectively. The phase is maximally advanced for $\phi > 0.7$, $\phi > 0.5$ and $\phi > 0.4$, respectively, when triggered by calcium pulses of 5, 2, and 1 pA, respectively. These calcium injections are small relative to the total inflow of calcium from the ER during a calcium transient ($\sim 35 \times 10^{-6}$ μmol) and through the membrane during an AP ($\sim 100 \times 10^{-6}$ μmol).

The dashed lines plotted in the bottom panels in Fig. 2 do not exactly represent the transitions of the phase changes but represent interpolations between subsequent points of the PRC curves for steps of 0.1. The PRCs in Fig. 2 show that an intracellular calcium oscillation and an AP are both capable of triggering an AP or calcium transient, respectively, except when they occur shortly after a preceding AP.

Entrainment of Calcium Oscillations of Two Cells by Electrical Coupling

Since IP_3 -mediated calcium oscillations and AP generation within a cell are tightly coupled processes (Fig. 2), electrical coupling between cells by gap junctions provides an indirect (electrical) coupling mechanism between IP_3 -mediated calcium oscillations in two neighboring cells. To investigate the role of gap junctions in the coupling of IP_3 -mediated calcium oscillations of two neighboring cells, we investigated the entrainment of two pacemaker cells with different intrinsic

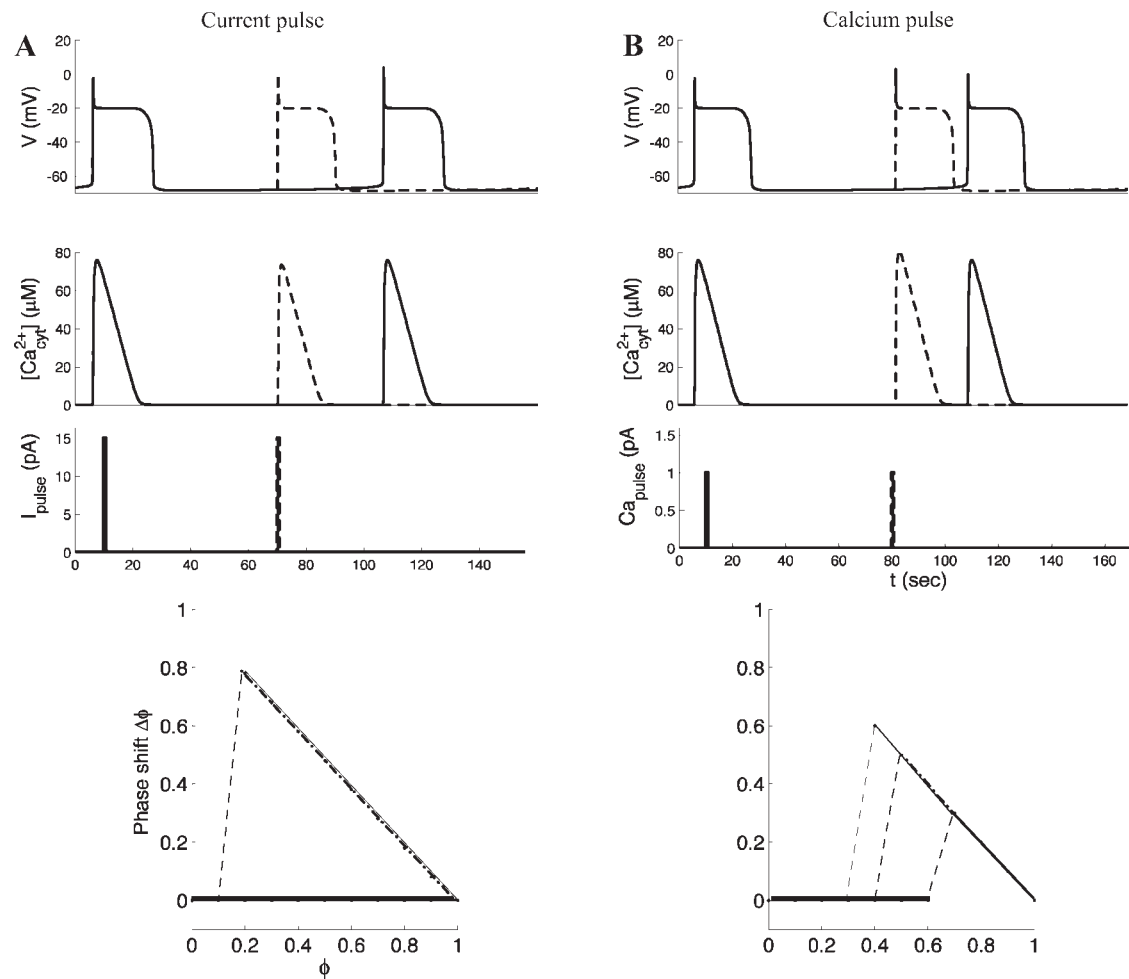


Fig. 2. Phase-response curves (PRC) of a single cell to depolarizing current pulses of 10, 15, and 20 pA of 50 ms in duration (A) and to calcium pulses associated with a calcium current injection of 1, 2, and 5 pA of 50 ms in duration (B). The top 3 subpanels show an example of the effect of current (15 pA in A) and calcium pulses (1 pA in B) on the phase advance of the action potential (AP) and calcium oscillations (dashed lines). Solid lines show the AP and calcium oscillations without perturbation. The bottom panels show the phase change of the inositol 1,4,5-trisphosphate (IP_3)-mediated calcium oscillator as a function of the timing of the current pulse (A) and calcium pulse (B). The bottom panel in A shows the phase change as a function of phase to a current pulse of 10 (thick solid line), 15 (dashed-dotted line), and 20 pA (thin solid line). The bottom panel in B shows the phase change as a function of phase to a calcium pulse of 1 (thick solid line), 2 (dashed-dotted line), and 5 pA (thin solid line). The dashed lines are linear interpolations between PRC values calculated at steps of 0.1.

frequencies (due to different IP_3 concentrations, $[\text{IP}_3]$) as a function of gap junctional conductance.

Figure 3 shows the major family of entrainment regions, commonly called Arnold tongues (34) (solid lines), as a function of the electrical coupling G_g . Notice that the vertical scale is in picosiemens. The entrainment regions are labeled by the ratio of the frequencies of the calcium oscillations of both cells: $f_2([\text{IP}_3]_{\text{cell 2}})/f_1([\text{IP}_3]_{\text{cell 1}})$. The $[\text{IP}_3]$ of cell 1 is set to a value of $1.0 \mu\text{M}$ (this value causes calcium oscillations at intermediate frequencies: $f_1 = 1/100 \text{ Hz}$), while the $[\text{IP}_3]$ of cell 2 is varied in steps of $0.005 \mu\text{M}$ at a rate of one step per 9,000 s from 0.0 to $8.0 \mu\text{M}$.

When two pacemaker cells are uncoupled ($G_g = 0$), the cells can only have (subharmonic) m/n frequency entrainment when the frequencies f_1 of cell 1 and f_2 of cell 2 are related by $mf_1 = nf_2$ (n and m integers). When the gap junctional conductance G_g increases in small steps, various modes of entrainment develop before complete synchrony (1:1 entrainment) is established. The value of G_g , where 1:1 entrainment develops, depends on the difference of the oscillation frequencies of the

two cells in the uncoupled mode. The regions where entrainment takes place are related by the relation $0 \leq |mf_1 - nf_2| < \epsilon(G_g, m, n)$, where ϵ increases for larger values of G_g . Figure 3 shows only the regions for the major entrainment ratios for f_2/f_1 (1:2, 2:3, 1:1, 4:3, and 3:2), but in between there are many much smaller regions with other ratios of m/n entrainment. The regions for various modes of entrainment grow with G_g and merge until a value of G_g is reached that gives 1:1 entrainment for all frequencies. For example, when we start at $G_g = 35 \text{ pS}$ and an IP_3 concentration of $0.4 \mu\text{M}$ for cell 2 (corresponding to an intrinsic oscillation frequency $f_2 = 1/190 \text{ Hz}$ for the cell in isolation), simulations reveal that this cell exhibits calcium transients at one-half the frequency of the calcium oscillations in cell 1. For increasing values of $[\text{IP}_3]$ in cell 2 at $G_g = 35 \text{ pS}$ (horizontal dashed line), the following major entrainment regions are observed: 1:2, 2:3, 1:1, 4:3, and 3:2, respectively. In between, there are many much smaller regions with other ratios of m/n entrainment. Figure 3 predicts that electrical coupling near 60 pS or higher between two cells with one cell having an $[\text{IP}_3]$ of $1.0 \mu\text{M}$ is sufficient to completely synchronize two

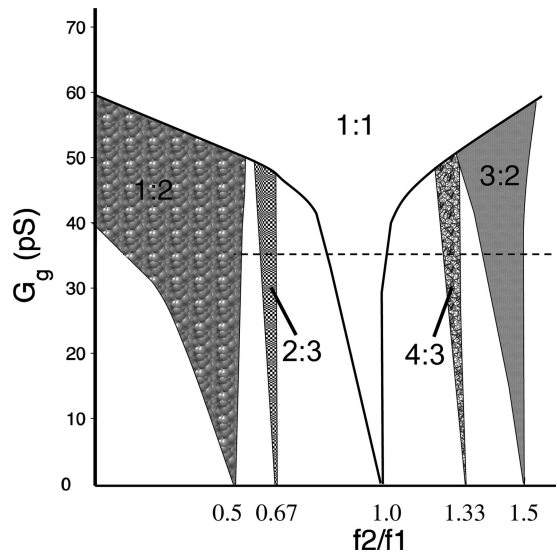


Fig. 3. Arnold tongues for 2 heterogeneous coupled cells as a function of the gap junction coupling conductance G_g . The $[IP_3]$ of the first cell is set to a value of $1.0 \mu\text{M}$, while the $[IP_3]$ of the second cell is varied in steps of $0.005 \mu\text{M}$ at a rate of one step per $9,000 \text{ s}$ from 0.0 to $8.0 \mu\text{M}$. It shows only the regions for the major entrainment ratios (1:2, 2:3, 1:1, 4:3, and 3:2).

heterogeneous NRK cells, irrespective of the IP_3 concentration in the second cell. In this range (for gap junctional conductance values above $\sim 60 \text{ pS}$), the cell with the lowest oscillation frequency locks to the cell with the highest oscillation frequency. Therefore, in the 1:1 entrainment region left from the ratio $f_2/f_1 = 1.0$, the frequency of the calcium oscillations is determined by the reference frequency f_1 and on the right side by the variable frequency f_2 .

From the results shown in Fig. 3, we infer that under conditions of a physiological gap junctional coupling strength of 3 nS between NRK cells (13), the intracellular calcium oscillations and APs of two oscillating NRK cells are fully synchronized. The fact that the fastest frequency always determines the synchronized frequency indicates that both calcium oscillators synchronize by phase resetting AP effects and not by continuous interaction (46, 49).

Synchronization of Cells in a Strand by Electrical Coupling

To explore the excitation of follower cells by pacemaker cells, we studied entrainment of a strand of follower cells by a terminal pacemaker cell. Since gap junctions allow diffusion of IP_3 , and because follower cells may be subject to stimulation of subthreshold IP_3 production, we assumed non-zero concentrations of IP_3 in the follower cells. For most simulations in this study, the follower cells have an $[IP_3]$ of $0.1 \mu\text{M}$, which does not give rise to spontaneous calcium oscillations. For the pacemaker cell, we chose an $[IP_3]$ of $1.0 \mu\text{M}$, which causes spontaneous calcium transients and APs (27).

Figure 4 shows the results of such an entrainment simulation. The solid and dashed lines demarcate different entrainment regions for a one-dimensional strand of follower cells with an $[IP_3]$ of 0.1 and $0.0 \mu\text{M}$, respectively, by a single terminal pacemaker cell ($[IP_3] = 1.0 \mu\text{M}$) as a function of the number of cells and G_g . Figure 4 shows that the mode of entrainment depends on the number of follower cells in the strand as well as the gap junctional conductance. For a single

pacemaker cell and one follower cell ($[IP_3] = 0.1 \mu\text{M}$), the minimal gap junctional conductance for full 1:1 entrainment is $\sim 0.06 \text{ nS}$. Increasing the number of cells for a fixed value for G_g at 0.1 nS changes the 1:118 entrainment to 1:2 entrainment for three cells and to 1:4 entrainment for four cells. For five or more cells, no synchronization takes place anymore when $G_g = 0.1 \text{ nS}$. Coupling in the range between 0.25 and 0.45 nS is sufficient for complete 1:1 synchronization of calcium oscillations and APs in a one-dimensional network of NRK cells with this IP_3 level, independent of the network size. If $[IP_3]$ in the follower cells is set to $0.0 \mu\text{M}$, the same results are obtained for these small values of G_g (Fig. 4, dashed lines superimposed on solid lines). Notice that experimental observations (13) report a gap junctional conductance for NRK cells of 3 nS , which is much larger than the optimal coupling range in our simulations (0.25 – 0.45 nS). We will come back to this topic in the DISCUSSION.

The entrainment regions are different in Fig. 4 for a strand of follower cells with an $[IP_3]$ of $0.1 \mu\text{M}$ (solid lines) and for a strand with cells set to $0 \mu\text{M}$ (dashed lines) for G_g values above 0.4 nS . For $[IP_3] = 0.1 \mu\text{M}$ in the follower cells, the entrainment changes from 1:2 to 1:3 and 1:4 for increasing values of G_g when the number of follower cells is larger than ~ 20 (solid line). For $[IP_3] = 0$, the IP_3 receptor in the follower cell is closed and AP transmission fails for G_g above 0.8 nS when the number of cells exceeds 30 cells (shaded area). Simulations reveal that the area marked with diagonal lines is where the entrainment is 1:3. The range of G_g values that allow 1:1 synchronization for a large number of cells is from ~ 0.25 to 0.4 nS .

These results demonstrate that small concentrations of IP_3 , which do not elicit spontaneous calcium oscillations, support synchronization of activity in networks of cells. For this reason, we used in this study an $[IP_3]$ of $0.1 \mu\text{M}$ for the follower cells to further investigate the interaction between IP_3 -mediated calcium oscillations and APs.

Summarizing, to completely synchronize a pacemaker and a single follower cell, a G_g near 0.06 nS is sufficient (Fig. 4), whereas for an infinitely long strand of cells, G_g must be in the

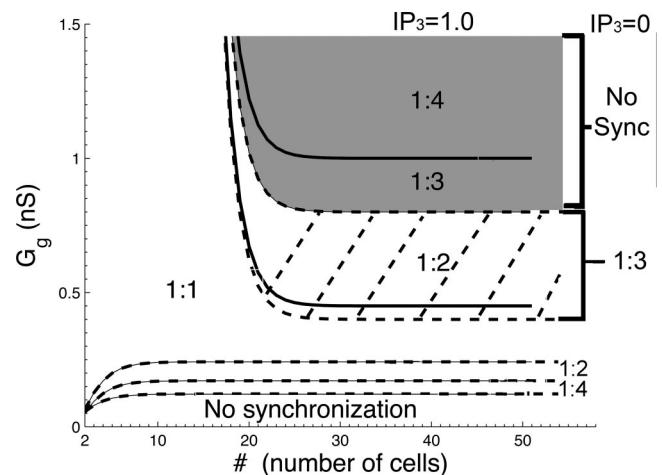


Fig. 4. Entrainment areas for a 1-dimensional network with 1 terminal pacemaker cell ($[IP_3] = 1.0 \mu\text{M}$) and follower cells (solid lines, $[IP_3] = 0.1 \mu\text{M}$; dashed lines, $[IP_3] = 0.0 \mu\text{M}$) as a function of the number of cells and G_g . No synchron, no synchronization.

range between 0.25 and 0.45 nS (Fig. 4). An explanation is given below.

The current from the pacemaker cell through the gap junctions to the follower cells is given by Eq. 2. Increasing the electrical coupling (G_g) increases the leak of current from the pacemaker cell to its neighbor cells. If the net current to a follower cell is large enough and fast enough, the membrane potential might approach the threshold value near -40 mV for L-type calcium channels. If that happens, the L-type calcium channels open, causing an AP and an inward current of calcium ions. The increase of calcium in the cytosol activates the IP₃ receptor, leading to a calcium transient.

An opposite effect of increasing the electrical coupling is that it decreases the equivalent impedance of the network. Since the equivalent impedance Z_{∞} for an infinitely large strand of follower cells decreases for increasing values of G_g ($\partial Z_{\infty} / \partial R_g > 0$ for all R_g ; see Eq. 5), decreasing R_g (increasing G_g) implies a smaller value for Z_{∞} . If the equivalent impedance of the network decreases, the available current from the pacemaker cell spreads to a larger number of follower cells in the network, which makes it harder for the pacemaker cell to depolarize its neighboring follower cell to the threshold of the L-type calcium channels for generation of an AP. In other words, a larger gap junction conductance leads to a decrease in the effective impedance and to a smaller net current from the pacemaker cell to its neighboring follower cell, which explains the shift from 1:1 to 1:2 entrainment for strong coupling ($G_g > 0.45$ nS) in Fig. 4 and to 1:4 entrainment for $G_g > 1.0$ nS for network sizes in the range of 20 cells and more.

In conclusion, small coupling conductances prohibit a sufficiently large current from the pacemaker to the follower cell to reach the membrane threshold for excitation. For a large conductance, the threshold for AP generation cannot be reached, since a large part of the current from the pacemaker to its neighboring follower cell flows to other follower cells, limiting the net current from pacemaker to its neighbor follower cell.

Entrainment and Propagation in a Strand of Electrically Well-Coupled NRK Cells

Failing AP transmission during strand entrainment. Figure 5 shows the results of a simulation of the membrane potential behavior of a pacemaker cell in isolation (A, thick solid line) and that of a pacemaker cell (B, thick solid line) coupled to 100 follower cells (thin solid lines) in a strand with a G_g of 3 nS. Note that this value for G_g is much larger than the values of G_g in Fig. 4. For $G_g = 3$ nS, the entrainment for a network of 20 cells or less is 1:1 and is 1:4 when the number of cells exceeds 30.

IP₃ concentrations are set to 1.0 and 0.1 μ M for the pacemaker and follower cells, respectively. As shown in Fig. 4, this situation corresponds to 1:1 for a small number of follower cells ($n < 17$) and corresponds to 1:4 entrainment for $n > 20$ cells. This means that one of every four calcium transients and APs generated by the pacemaker cell results in AP and calcium transients in the strand of follower cells. Figure 5B shows an example where propagation does not take place. Figure 6 shows a case where propagation does occur.

In Fig. 5A, the uncoupled pacemaker cell (thick solid line) has an AP with a peak voltage near $+10$ mV, followed by a plateau phase near -20 mV. The AP is triggered by Ca²⁺ release from the ER store through the IP₃ receptor (Fig. 5E). The increased $[Ca^{2+}]_{\text{cyt}}$ (Fig. 5C) causes depolarization of the cell by activation of the Cl_{Ca} channels. This depolarization to the Nernst potential of the Cl_{Ca} channels near -20 mV activates the L-type calcium channel (Fig. 5, G and I), which leads to a further increase in $[Ca^{2+}]_{\text{cyt}}$ (Fig. 5C).

Figure 5, right, shows the results when the pacemaker is coupled to 100 follower cells. Comparing the left and right panels reveals some important differences between the results for an uncoupled pacemaker cell and for a pacemaker cell coupled to a strand of follower cells. The main difference relates to the slow and small increase of $[Ca^{2+}]_{\text{cyt}}$ in the

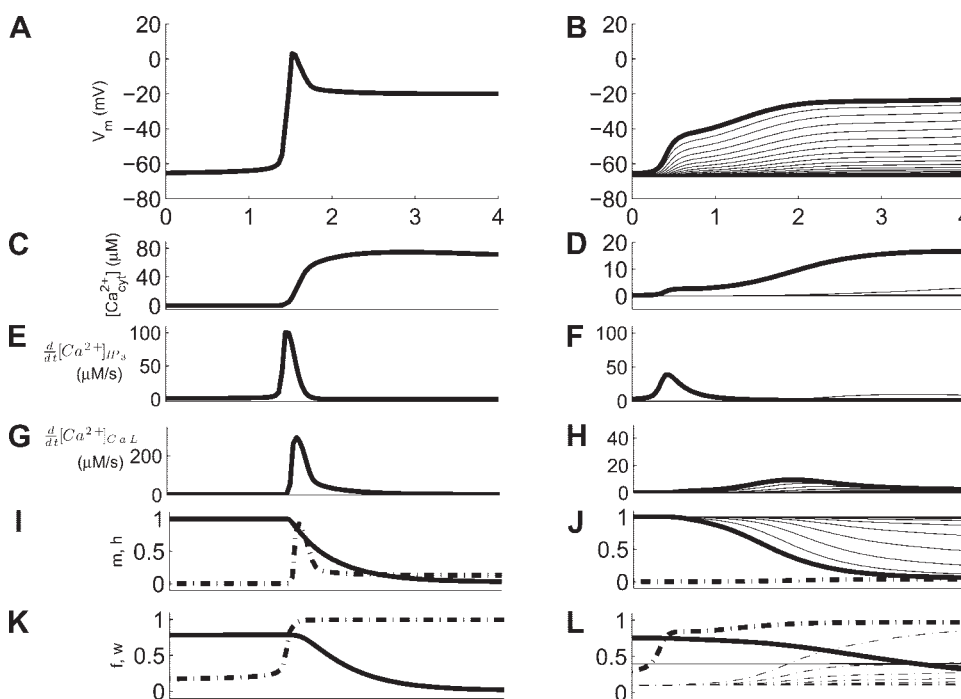


Fig. 5. Membrane potential (V_m ; A and B), cytosolic calcium concentration ($[Ca^{2+}]_{\text{cyt}}$; C and D), calcium flow through the IP₃ receptor (E and F), calcium flow through the L-type calcium channels (G and H), and the fraction of open activation (m , thick dashed-dotted line) and inactivation gates (h , thick solid line; I and J) for an isolated pacemaker cell (thick solid lines, left panels) and for a pacemaker cell (thick solid lines, right panels) coupled to 100 follower cells (thin solid lines). The fraction of open activation (f , thin dashed-dotted line) and inactivation gates (w , thin solid line) of the IP₃ receptor for a pacemaker cell in K and L are shown coupled to 100 follower cells (f , thin dashed-dotted line; w , thin solid line; $G_g = 3$ nS) in L. $d[Ca^{2+}]_{\text{IP}_3}/dt$ and $d[Ca^{2+}]_{\text{CaL}}/dt$ represent the change in calcium concentration due to calcium inflow through the IP₃ receptor and the L-type calcium channel, respectively.

pacemaker cell (compare Fig. 5, *C* and *D*, thick solid line) and the corresponding slow and small depolarization of the membrane potential (compare Fig. 5, *A* and *B*) in the coupled situation for the pacemaker cell. Coupling the pacemaker cell to its neighboring follower cells by gap junctions causes the current from the pacemaker cell to leak away to the follower cells. As a result, depolarization of the membrane potential of the pacemaker cell by the Cl_{Ca} channels reaches a lower peak value (Fig. 5*B*), and the level of activation of the L-type calcium channels of the pacemaker cell is not as high as in the case of the isolated pacemaker cell. This becomes clear by comparing the data in Fig. 5, *I* and *J*, which show the activation gate (m ; thick dashed-dotted line) and inactivation gate (h ; thick solid line) for the uncoupled and coupled situation, respectively. For the uncoupled pacemaker cell, the m gates open (Fig. 5*I*), which does not happen for the coupled pacemaker cell (Fig. 5*J*), leading to AP failure in the strand. As a consequence of the small activation of the L-type calcium channels in the coupled pacemaker cell, there is hardly any calcium inflow through the L-type calcium channels into the cytosol (compare Fig. 5, *G* and *H*, and notice the different scales of the vertical axes). This also affects the boosting of CICR by activation of the IP_3 receptor, because the smaller inflow of calcium through the L-type calcium channel weakens CICR and results in a slower and smaller calcium flow through the IP_3 receptor (compare Fig. 5, *E* and *F*) for the coupled pacemaker.

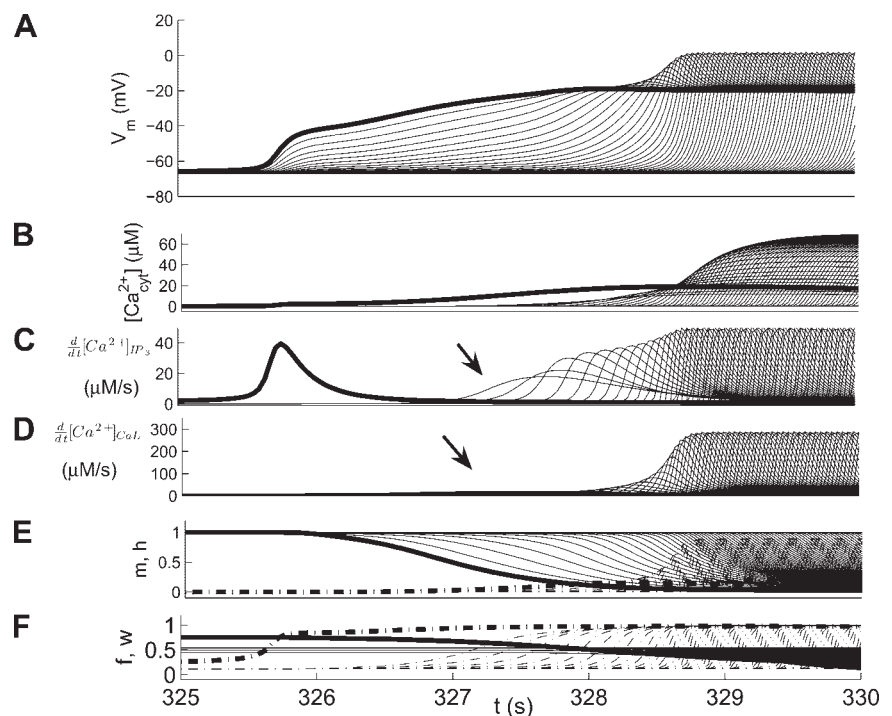
For the isolated pacemaker cell, the fraction of open activation gates (f ; thick dashed dotted line) increases rapidly, followed by a slow closure of the inactivation gates (w ; thick solid line in Fig. 5*K*). When the pacemaker is coupled to a strand of 100 follower cells the fraction of open activation gates does not reach as high values as for the isolated pacemaker (compare thick dashed-dotted lines in Fig. 5, *K* and *L*). Notice that the fraction of open inactivation gates (w) is near 0.4 for the

follower cells (thin solid lines in *L*, which all superimpose). The gate is not yet completely deactivated after the previous AP, which has implications for the propagation of the AP, as we will show when we compare Figs. 5 and 6.

In summary, when the pacemaker cell is coupled to a linear strand of follower cells, the membrane potential of the pacemaker cell increases much more slowly than in the uncoupled case and does not reach values as high during the plateau phase due to the decreased flux of calcium ions through the L-type calcium channels and IP_3 receptor of the pacemaker cell. The depolarization of the follower cells due to electrical coupling activates the L-type calcium channels in the follower cells only to a very small extent (Fig. 5*J*) and causes only a very small inflow of calcium ions (Fig. 5*H*). This inflow is too small to induce a significant CICR through the IP_3 receptor in the follower cells (thin solid line in Fig. 5*F*), because w is not yet sufficiently deactivated. As a consequence, a single pacemaker cell is not powerful enough to supply 1:1 entrainment between AP propagation and calcium oscillations in a strand of NRK cells with $[IP_3] = 0.1 \mu M$.

Entrained AP transmission. Figure 6 shows the propagation of activity for a pacemaker cell coupled to 100 follower cells with a G_g of 3 nS when the pacemaker cell succeeds in triggering AP propagation in the follower cells. In Fig. 6*A*, the coupled pacemaker cell (thick solid line) depolarizes to -20 mV. This depolarization is triggered by calcium release from the store through the IP_3 receptor (Fig. 6*C*). The increased $[Ca^{2+}]_{cyt}$ causes depolarization of the cell by activation of the Cl_{Ca} channels. Note that the rise of the membrane potential for the pacemaker cell and its neighboring follower cells is much slower than that for distant follower cells. This causes a gradual start of the inactivation of the L-type calcium channel (decreasing h ; solid lines in Fig. 6*E*) before activation m increases (dashed-dotted lines). Since the activation m in the pacemaker cell hardly increases above the value zero (thick

Fig. 6. Membrane potential (*A*), $[Ca^{2+}]_{cyt}$ (*B*), calcium flow through the IP_3 receptor (*C*), calcium flow through the L-type calcium channel (*D*), and the fraction of open activation (m , dashed lines) and inactivation gates (h , solid lines; *E*) for a pacemaker cell (thick lines) coupled ($G_g = 3$ nS) to 100 follower cells (thin lines). The fraction of open activation (f , thick dashed-dotted line) and inactivation gates (w , thick solid line) of the IP_3 receptor for a pacemaker cell coupled to 100 follower cells (f , thin dashed-dotted lines; w , thin solid lines) is shown in *F*. Arrows indicate where a small inflow of calcium by the L-type calcium channel (*D*) causes a small calcium-induced calcium release (CICR) through the IP_3 receptor (*C*). Note the different scales for calcium flow in *C* and *D*.



dashed-dotted line in Fig. 6E), the L-type calcium channels in the pacemaker cell hardly open (Fig. 6D). For more distant follower cells, the rise of the membrane potential is much faster and activation m of the L-type calcium channel increases rapidly, resulting in an AP.

The depolarization of the pacemaker cell to the Nernst potential of the Cl_{Ca} channels near -20 mV activates the L-type calcium channels in the neighboring follower cell slightly (hardly visible in Fig. 6D, see arrow), causing a small inflow of calcium ions. Although the inflow of calcium in the follower cells is small and hardly visible in Fig. 6D, the fraction of open inactivation gates (w) of the IP_3 receptor (solid lines in Fig. 6F) is large enough to allow a significant CICR through the IP_3 receptor (Fig. 6C, see arrow). Moreover, the $[\text{Ca}^{2+}]_{\text{cyt}}$ (Fig. 6B) due to small influx through the L-type calcium channel (Fig. 6D) and through the IP_3 receptor (Fig. 6C) is large enough to cause full depolarization to the Nernst potential of the Cl_{Ca} channels (Fig. 6A). The CICR through the IP_3 receptor in each follower cell reinforces the speed of their depolarization and, therefore, contributes to a better and stronger AP propagation in the one-dimensional array of cells.

The fractions of open activation (f ; thick dashed-dotted lines) and inactivation gates of the IP_3 receptor for a pacemaker cell (w ; thick solid line) coupled to 100 follower cells (w ; thin solid lines) are shown in Fig. 6F. Notice that the fraction of open w gates for the neighboring follower cells is a little higher than in Fig. 5K (thin solid lines). This is due to the small $[\text{IP}_3]$ of $0.1 \mu\text{M}$ (see Eq. A23), which gives a long time constant τ_w for deactivation. It takes ~ 300 s to reopen the inactivation gate w of the follower cells completely. Since the pacemaker cell generates an AP every 90 s, the inactivation gate w of the follower cells after a calcium transient has not recovered sufficiently at the next AP of the pacemaker cell. This is clear in Fig. 5F, where the inactivation gate of the neighboring follower cell is 0.4, whereas it reaches values near 0.5 and 0.6 in Fig. 6F (thin solid lines).

The main difference between Figs. 5 and 6 is that the inactivation gate w (thin solid lines) of the IP_3 receptor in the follower cells has recovered to higher values in Fig. 6F than in Fig. 5K. Therefore, the relatively small inflow of calcium ions through the L-type calcium channels is large enough to activate the IP_3 receptor by CICR in the first follower cell (see arrow, Fig. 6C). The same occurs in the other follower cells. The membrane potential exerts a positive feedback on the calcium oscillator through calcium influx through L-type calcium channels. On the other hand, the release of calcium through the IP_3 receptor exerts a positive feedback on the depolarization of the membrane. As a result, AP propagation with underlying calcium oscillations is generated in the follower cells. This positive interaction between membrane excitability and IP_3 receptor explains why a small amount of IP_3 in the cell supports synchronization and propagation of activity in a network of cells.

We can understand the 1:4 entrainment of AP propagation (Figs. 5 and 6) by having a closer look at the deactivation time constant τ_w for the w gate. The time constant τ_w (Eq. A23) determines the time for deactivation (w) of the IP_3 receptor, which depends among other things on $[\text{IP}_3]$. For low $[\text{IP}_3]$ values (near $0.1 \mu\text{M}$) in the follower cells, the time constant τ_w of the inactivation gate w of the IP_3 receptor is long (in the order of 300 s). For high $[\text{IP}_3]$ values (near $1.0 \mu\text{M}$) in the

pacemaker cell, τ_w is shorter and about 90 s. Since the time constant τ_w in the follower cells is long (about 300 s) relative to the time interval between APs generated by the pacemaker cell (about 90 s), the deactivation of the IP_3 receptor in the follower cells has not yet recovered after an AP and IP_3 -mediated calcium oscillation when the pacemaker cell generates the next AP. This explains why 1:1 synchronization between pacemakers and followers is not possible in this case and why synchronization becomes harder for smaller amounts of IP_3 in the cell.

Propagation in a strand of cells. We now address the experimental observation that APs and calcium oscillations are propagated with a G_g that is much larger (3 nS) than the predicted optimal gap junctional coupling range for synchronization of a pacemaker to followers (range 0.25–0.4 nS in Fig. 4). We have to keep the following in mind: if the gap junction conductance is very small, the current from the pacemaker to the follower cell is too small to depolarize its neighbor cell rapidly and to a sufficiently high membrane potential. If the gap junction conductance is very large, the pacemaker cell is not able to provide enough current for depolarization of its neighboring cell, since most of the current flows through the network to other cells. As we will show, robust AP propagation and excitation of follower cells in the latter case can be achieved in the model in two ways: by increasing the conductance of the L-type calcium channels and by increasing the number of pacemaker cells.

The first solution is to increase the conductance G_{CaL} of the L-type calcium channel, which is helpful for both the pacemaker and the follower cells. With increased values of G_{CaL} , depolarization of the membrane potential of the pacemaker cell leads to a larger current through the L-type calcium channels and to more current through the gap junctions. This generates a larger current from pacemaker to follower cells and makes it easier to reach the threshold level for opening of L-type calcium channels in the follower cells. For follower cells, a larger opening of their L-type calcium channels leads to better facilitation of CICR through the IP_3 receptor. However, since it is known that the maximal value for G_{CaL} is close 1.6 nS (15), it would not be realistic to set G_{CaL} to values higher than 1.6 nS, used in this study.

The second solution is to increase the number of terminal pacemaker cells in the one-dimensional network, which contributes to a larger current to the follower cells. When enough pacemakers are placed in the network, 1:1 AP propagation is observed. This is illustrated in Fig. 7, which shows the result of a simulation of a coupled strand with three terminal pacemakers ($[\text{IP}_3] = 1.0 \mu\text{M}$) and 100 follower cells ($[\text{IP}_3] = 0.1 \mu\text{M}$). The release of calcium from the ER to cytosol by the IP_3 receptor in the pacemaker cells (Fig. 7C) activates the Cl_{Ca} channels, causing a depolarization to -20 mV (Fig. 7A). This depolarization activates the L-type calcium channels (Fig. 7D). Note the delay of the fluxes through the L-type calcium channels (Fig. 7D) relative to the fluxes through the IP_3 receptor (Fig. 7C). The depolarization of the three pacemaker cells causes a depolarization of the follower cells (Fig. 7A) and APs by activation of the L-type calcium channels of the followers (Fig. 7D). The three pacemakers cause 1:1 entrainment for the full network with 100 followers.

Differences in pacemaker and follower cells. Comparison of the behavior of the pacemaker cells and the follower cells in

Fig. 7. Membrane potential (A), $[Ca^{2+}]_{cyt}$ (B), calcium flow through the IP₃ receptor (C), and calcium flow through the L-type calcium channel (D) for a 1-dimensional network with 3 pacemaker cells (thick solid lines) coupled to 100 follower cells (thin solid lines). $[IP_3]$ is set to 1.0 and 0.1 μ M for the pacemaker and follower cells, respectively.

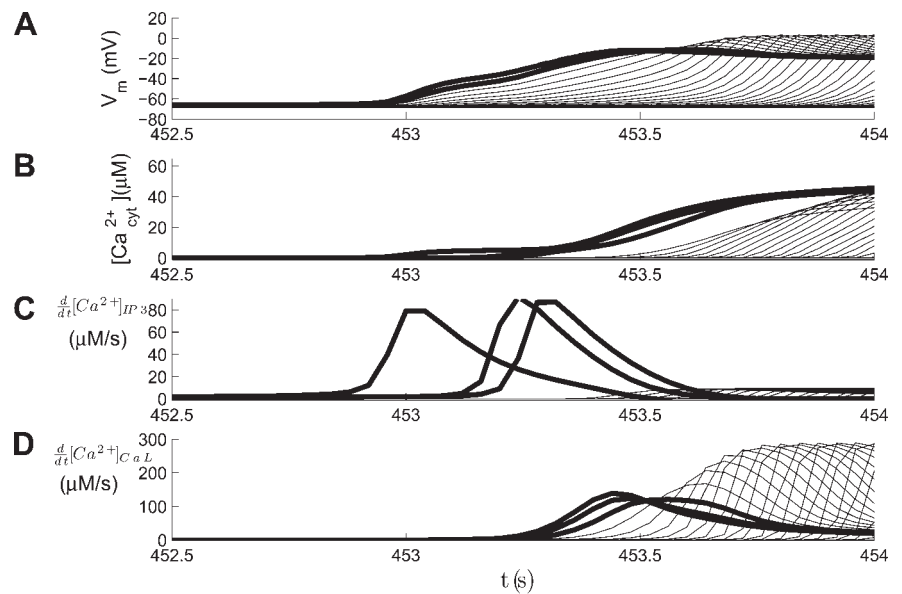


Fig. 7 shows some important differences. The first difference to be mentioned is the smaller peak of the AP in the pacemaker cells than in the follower cells (see Fig. 7A, compare thick solid lines with thin solid lines). In a pacemaker cell, APs are triggered by IP₃-mediated intracellular calcium oscillations. Each calcium transient leads to opening of the Cl_{Ca} channels, causing a depolarization of the pacemaker cell to the chloride Nernst potential near -20 mV. This depolarization opens the L-type calcium channels, which have a reversal potential near 50 mV. Since the calcium filling of the cytosol by release of calcium from the stores (see Fig. 7C) and the corresponding depolarization to -20 mV due to activation of the chloride channels is slow (see Fig. 7A) relative to the activation and inactivation time constants of the L-type calcium channel, inactivation of the L-type calcium channels starts during the depolarization to -20 mV. This explains why the inflow of calcium through the L-type calcium channel (Fig. 7D) and the initial peak of the AP are smaller in pacemaker cells than in follower cells. The inward calcium flow through the L-type calcium channels (Fig. 7D) is approximately twice as small for pacemaker cells as for follower cells. Figure 7 illustrates that three pacemaker cells are able to initiate propagating activity in a linear strand of follower cells, in which each has a small concentration of IP₃ (0.1 μ M) that assists in AP propagation through the network.

In Fig. 4 we showed that a single pacemaker could not induce propagating activity in a linear strand with a large number of follower cells for large gap junctional conductance. With three pacemakers, 1:1 entrainment is obtained for gap junctional conductances G_g above 0.25 nS.

Minimal value for G_{CaL} . As explained above, L-type calcium channels are necessary for propagation of activity in a network of NRK fibroblasts (7). Figure 8 shows the simulation results where we tried to find the minimum number of pacemaker cells as a function of G_{CaL} at a constant gap junction conductance of 3 nS. The minimal number of pacemaker cells required for stable 1:1 propagation of APs in a linear array of follower cells decreases for increasing G_{CaL} . The data points of the simulations in Fig. 8 reveal that no AP propagation is

possible for G_{CaL} below 1.45 nS. Therefore, in our model, a critical minimal value for G_{CaL} is necessary for AP propagation in a network.

DISCUSSION

The aim of this model study was to investigate how electrical coupling of excitable cells with IP₃-mediated calcium oscillations affects the initiation and propagation of calcium waves in a strand of cells. IP₃-mediated calcium oscillations in two neighboring cells were coupled to the excitable membrane by cytosolic calcium as in the study by Imtiaz et al. (22). Our general conclusion is that the interaction between IP₃-mediated calcium oscillations and APs in electrically coupled NRK cells provides a mechanism for fast calcium wave propagation and synchronization, in which the CICR component plays a significant supportive role.

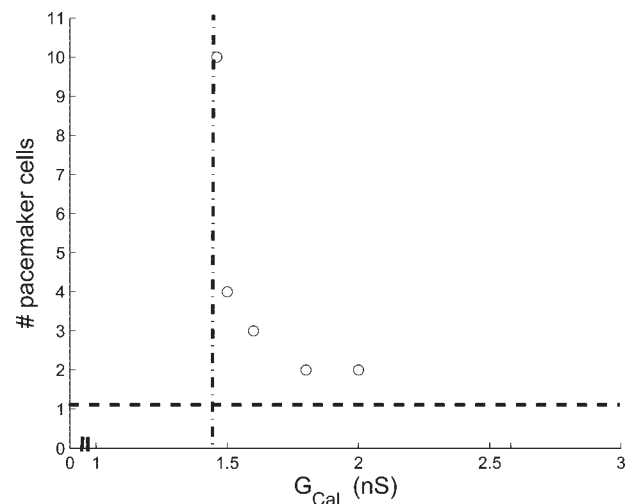


Fig. 8. Simulation results (\circ) for 1:1 synchronization and propagation of APs as a function of the conductance of the L-type calcium channel (G_{CaL}) and number of pacemaker cells for a constant G_g of 3 nS. No propagation takes place for $G_{CaL} < 1.4$ nS whatever the number of pacemaker cells.

Role of Electrical Coupling Strength

The main result of this study is that it emphasizes the important functional role of the coupling between the excitable membrane and CICR from intracellular stores for calcium APs and the important role of electrical coupling between cells for the initiation and propagation of calcium APs. These results provide a better understanding of empirical results by Yao and Parker (48), who concluded that “electrical transmission may provide a means to ‘leapfrog’ slow chemical wave transmission and rapidly synchronize Ca^{2+} release within large individual cells and across populations of electrically coupled cells.” A similar idea was reached by Sanders et al. (37), who concluded, on the basis of a large set of empirical data, that “voltage-dependent Ca^{2+} entry that increases Ca^{2+} activity in pacemaker units near IP_3 receptors may be responsible for coordination of Ca^{2+} release events and entrainment of unitary currents within a network of ICC.”

Figure 3 shows entrainment for two heterogeneous pacemaker cells, which display full synchronization of intracellular calcium oscillations for a coupling conductance (G_g) above 60 pS, which is well in agreement with Imtiaz et al. (22), who found that weak electrical coupling is sufficient to synchronize heterogeneous cells of cell pairs. This result explains that at the physiological gap junctional coupling strength (3 nS) of NRK cells (14), the intracellular calcium oscillations and APs of two oscillating cells are completely synchronized in phase. In the modeling study by Imtiaz et al. (22), it was reported that anti-phase behavior could occur for two weakly coupled cells for high oscillation frequencies, which is a well known result for interacting oscillators (9). This anti-phase coupling in their study is the result of the time constants involved in voltage-dependent IP_3 synthesis. Since it takes some time before changes in the membrane potential affect the production of IP_3 , the effective coupling between cells by voltage-dependent IP_3 production has a frequency-dependent delay. Therefore, we conclude that voltage-dependent IP_3 synthesis cannot play an important role, since it would disable synchronization between cells to form a pacemaker cluster.

For low-frequency intracellular calcium oscillations (typically 1 cycle/min or lower), this delay is small relative to the period of the calcium oscillations, which results in in-phase behavior. For high-frequency intracellular calcium oscillations (2 cycles/min or higher), the period of calcium oscillations is small relative to the time constant for production of IP_3 , resulting in out-of-phase oscillations. In NRK cells, the highest oscillation frequencies are near 1 cycle/min, but in general, the oscillation frequency is much lower. Therefore, out-of-phase synchronization due to voltage-dependent IP_3 production does not happen in NRK cells, and therefore, we did not include voltage-dependent IP_3 production.

Figure 4 shows that synchronization of follower cells by a pacemaker cell is easier if the follower cells have a non-zero concentration of IP_3 , allowing calcium transients by CICR. The CICR through the IP_3 receptor in each follower cell reinforces the speed of its depolarization and, therefore, contributes to a better and stronger AP propagation in the one-dimensional array of cells. Moreover, Fig. 4 shows that entrainment and synchronization is optimal for a coupling between 0.25 and 0.45 nS, whereby 1:1 propagation of APs in the network is facilitated. However, the actual conductance of gap junctions

between NRK cells is ~ 3 nS, which is much larger than the optimal coupling range that follows from Fig. 4. In our view, the relatively high conductance of 3 nS has at least two consequences.

The first one is that it prevents initiation of activity by a single pacemaker but allows synchronized activity of a small cluster of pacemaker cells. It prevents spontaneous random activity by a single pacemaker cell and ensures robust initiation by a small cluster. For a linear strand, at least three pacemakers are sufficient for propagation. Pilot studies for a two-dimensional network show that roughly 300 pacemaker cells are necessary to initiate propagating activity.

The second aspect related to the gap junctional conductance relates to the velocity of propagation. A larger gap junctional conductance gives a larger propagation velocity (36). Previous studies on propagation of activity in a network of nonexcitable cells with IP_3 -mediated calcium oscillations (10, 19, 20, 40) have shown that propagation may occur via diffusion of calcium and/or IP_3 through the gap junctions. Since diffusion is relatively slow relative to electrical coupling, the propagation velocity in such a network is typically in the range from 5 to 50 $\mu\text{m/s}$ (19, 35, 38), which is much slower than propagation in excitable cells (typically 0.5–100 cm/s) and in our NRK cells (6, 16), where the propagation velocity is approximately a few millimeters per second.

Required Number of Pacemaker Cells for Exciting the Strand

The analysis of the one-dimensional network in Figs. 5 and 6 with physiological electrical coupling ($G_g = 3$ nS) reveals that one terminal pacemaker cell cannot deliver sufficient current to the follower cells to obtain 1:1 synchronization and AP propagation in the cell strand. Increasing the value of L-type calcium conductance (G_{CaL}) alone would not help (see Fig. 8). The minimal number of pacemaker cells required to initiate AP propagation depends on the $[\text{IP}_3]$ of the follower cells (compare results for $[\text{IP}_3] = 0$ and $[\text{IP}_3] = 0.1 \mu\text{M}$ in follower cells in Fig. 4) and critically depends on G_{CaL} , which needs to be larger than 1.45 nS to facilitate propagation of APs at all (Fig. 8). In this study we have fixed G_{CaL} at 1.6 nS, which results in a requirement of three pacemaker cells for 1:1 propagation of APs in the one-dimensional network.

Chemical Coupling Versus Electrical Coupling

We have shown that calcium waves and propagation of APs can be achieved by a mechanism where depolarization by AP firing and calcium-triggered opening of chloride channels cause an AP and intracellular calcium transient in its neighbor cell. Such a coupling mechanism is significantly more effective than that of the chemical coupling-based class of models, since a membrane potential change has a quick coupling effect over distances several orders of magnitude greater than diffusion of either calcium or IP_3 through gap junctions (40).

Both calcium and IP_3 have been shown to permeate through gap junctions by diffusion. This mechanism plays a crucial role in the propagation of calcium waves in networks with nonexcitable cells (10, 19, 20, 40). In our study with excitable cells, the electrical coupling and the relatively fast dynamics of the L-type calcium channel provide a much faster propagation than in nonexcitable cells. Since diffusion of calcium and IP_3

takes place on a time scale much longer than the time scale of propagation by electrical coupling and activation of the L-type calcium channels, we have not incorporated diffusion of calcium and IP₃ in our study.

In a recent study, Tsaneva-Atanasova et al. (43) suggested that intercellular calcium diffusion is necessary and sufficient to synchronize the oscillations in neighboring cells with different intrinsic oscillation frequencies. The results of our study indicate that intercellular calcium diffusion may be sufficient but is not necessary, since coupling of intracellular calcium oscillations by the excitable membrane and electrical intercellular coupling also achieves synchronization of pacemaker cells with different intrinsic oscillation frequencies.

Several studies (see e.g., Ref. 19) calculated the minimal gap junctional permeability for calcium, which is required for calcium wave propagation, as a function of the diffusion coefficient for calcium. The minimal value is found to be ~0.05 μm/s, which gives an inflow of about 0.25×10^{-6} μmol in our cell. The results of our model study show that the total change of [Ca²⁺]_{cyt} due to inflow through the L-type calcium channels is about 100×10^{-6} μmol per AP. This is much larger than the change due to diffusion of calcium, which explains why the propagation of calcium waves mediated by the L-type calcium channels is faster and more robust. In the present model study, agonist or IP₃ diffusion may improve local synchronization of the surrounding follower cells by smoothing the sensitivities of the CICR mechanism.

Voltage-Dependent Gap junctional Conductance

In our study, the gap junctional conductance is assumed to be independent of the voltage of the membrane. However, it is well known that the gap junctional conductance is not constant but voltage dependent. The gap junctional conductance between two cells may decrease up to 20% during an AP compared with the steady-state conductance without any voltage difference across the gap junction. In a recent study using transfected neuroblastoma cells, inactivation kinetics of Cx43 were studied by imposing an AP clamp instead of a rectangular voltage pulse on one of the cells (30). These experiments showed that following the peak of the AP, the junctional conductance decreased within 25 ms to 58% of control. These relatively slow time constants are in agreement with experimental observations (2), which indicate that the transition rates for the gap junction channels are significantly longer than the time constant of the cell membrane, which is ~1 ms. Comparison of these inactivation times to transjunctional conduction times observed during steady-state propagation under conditions of severe uncoupling suggests that gap junctional gating has only a minor effect on overall conduction velocities (36).

Functional Implications

The results of this study show that the coupling of intracellular calcium oscillations and AP firing causes propagation of activity through a network of cells, which is robust and much faster than propagation of calcium waves in a network of nonexcitable cells (12, 19, 20, 43).

CICR through the IP₃ receptor, triggered by calcium inflow through L-type calcium channels during an AP, supports cell depolarization by activation of Cl_{Ca} channels. This boosting of propagation of activity by CICR provides a robust mechanism

that is also found in gastrointestinal cells (44), urethral cells (4, 22), and heart pacemaker cells (31). In all these cell types, robust pacemaking and propagation of activity is crucially important for the function of the cell network in the organism.

In smooth muscle cells, oscillatory release of calcium through IP₃ receptors and voltage-dependent calcium inflow through L-type calcium channels underlie rhythmic vasomotion (1, 50). Spontaneous calcium waves occurring after a long AP plateau may also modulate the removal of voltage-dependent inactivation of L-type calcium channels and affect the likelihood of the occurrence of early afterdepolarizations (48). Spontaneous calcium oscillations may be implicated in diverse manifestations of heart failure-impaired systolic performance, increased diastolic tonus, and an increased probability of the occurrence of arrhythmias (48). Therefore, the outcomes of this model study are also of interest for understanding mechanisms of pacemaker synchronization and AP propagation in many other systems.

Conclusion

Consistent with experimental observations for NRK cells (30), we have shown that electrical intercellular coupling is sufficient for synchronizing calcium oscillations of pacemaker cells and for propagation of action AP-coupled calcium waves over a linear network of cells. For NRK cells it has become clear that membrane excitation can evoke and enhance release of calcium from the ER store via voltage-dependent calcium inflow through L-type calcium channels. Our general message is that some form of CICR interaction with or caused by calcium inflow through voltage-dependent calcium channels can boost propagation of electrical excitation and its continuous calcium oscillations. Any form of CICR (ryanodine-mediated receptors are another example) would engage a similar interaction.

APPENDIX

Equations

This appendix gives an overview of the equations that are relevant for the dynamics of the membrane potential and intracellular calcium oscillation. For further details, see Kusters et al. (27).

$$C_m \frac{dV_m}{dt} = -(I_{Kir} + I_{leak} + I_{CaL} + I_{Cl(Ca)} + I_{SDC}) \quad (A1)$$

$$I_{Kir} = G_{Kir} \sqrt{\frac{K_0}{K_{ost}}} \left(\frac{\alpha}{\alpha + \beta} \right) (V_m - E_K) \quad (A2)$$

$$\alpha = \frac{0.1}{1 + \exp[0.06(V_m - E_K - 50)]} \quad (A3)$$

$$\beta = \frac{3 \times \exp[0.0002(V_m - E_K + 100)] + \exp[0.0002(V_m - E_K - 10)]}{1 + \exp[-0.06(V_m - E_K - 50)]} \quad (A4)$$

$$E_K = 1,000 \frac{RT}{F} \ln \left(\frac{K_0}{K_i} \right) \quad (A5)$$

$$I_{leak} = G_{leak} (V_m - E_{leak}) \quad (A6)$$

$$I_{CaL} = mhG_{CaL} (V_m - E_{CaL}) \quad (A7)$$

$$m_{\infty} = \frac{1}{1 + \exp\left(-\frac{V_m + 10}{5.24}\right)} \quad (A8)$$

$$\tau_m = 0.005 \frac{m_{\infty}[1 - \exp(-(V_m + 10)/5.9)]}{0.035(V_m + 10)} \quad (A9)$$

$$h_{\infty} = \frac{1}{1 + \exp\left(\frac{V_m + 37}{4.6}\right)} \quad (A10)$$

$$\tau_h = \frac{0.02}{0.02 + 0.0197 \exp\{-[0.0337(V_m + 10)]^2\}} \quad (A11)$$

$$I_{Cl(Ca)} = \frac{[Ca^{2+}]_{cyt}}{[Ca^{2+}]_{cyt} + K_{Cl(Ca)}} G_{Cl(Ca)} (V_m - E_{Cl(Ca)}) \quad (A12)$$

$$I_{SDC} = \frac{K_{SDC}}{[Ca^{2+}]_{cyt} + K_{SDC}} G_{SDC} (V_m - E_{SDC}) \quad (A13)$$

$$\frac{d[BCa]}{dt} = k_{on}([T_B] - [BCa])[Ca^{2+}]_{cyt} - k_{off}[BCa] \quad (A14)$$

$$J_{PM} = -\frac{10^{-6}}{z_{Ca} F A_{PM}} (I_{CaL} + I_{SDC}) - J_{PMCA} \quad (A15)$$

$$J_{PMCA} = J_{PMCA}^{max} \frac{[Ca^{2+}]_{cyt}}{[Ca^{2+}]_{cyt} + K_{PMCA}} \quad (A16)$$

The equations defining the properties of the IP₃-mediated intracellular calcium dynamics are as follows:

$$Vol_{cyt} \frac{d[Ca^{2+}]_{cyt}}{dt} = A_{ER}(J_{leak ER} + J_{IP_3R} - J_{SERCA}) - \frac{d[BCa]}{dt} Vol_{cyt} + A_{PM} J_{PM} \quad (A17)$$

$$Vol_{ER} \frac{d[Ca^{2+}]_{ER}}{dt} = A_{ER}(-J_{leak ER} - J_{IP_3R} + J_{SERCA}) \quad (A18)$$

$$J_{leak ER} = K_{leak ER}([Ca^{2+}]_{ER} - [Ca^{2+}]_{cyt}) \quad (A19)$$

$$J_{IP_3R} = f_{\infty}^3 w^3 K_{IP_3R}([Ca^{2+}]_{ER} - [Ca^{2+}]_{cyt}) \quad (A20)$$

$$f_{\infty} = \frac{[Ca^{2+}]_{cyt}}{K_f IP_3 + [Ca^{2+}]_{cyt}} \quad (A21)$$

$$w_{\infty} = \frac{\frac{[IP_3]}{K_{wIP_3} + [IP_3]}}{\frac{[IP_3]}{K_{wIP_3} + [IP_3]} + K_{w(Ca)}[Ca^{2+}]_{cyt}} \quad (A22)$$

$$\tau_w = \frac{a}{\frac{[IP_3]}{K_{wIP_3} + [IP_3]} + K_{w(Ca)}[Ca^{2+}]_{cyt}} \quad (A23)$$

$$J_{SERCA} = J_{SERCA}^{max} \frac{([Ca^{2+}]_{cyt})^2}{([Ca^{2+}]_{cyt})^2 + K_{SERCA}^2} \quad (A24)$$

GRANTS

This research project was funded by The Netherlands Organization for Scientific Research (NWO Project 805.47.066).

REFERENCES

1. **Aalkjaer C, Nilsson H.** Vasomotion: cellular background for the oscillator and for the synchronization of smooth muscle cells. *Br J Pharmacol* 144: 605–616, 2005.

2. **Baigent S.** Cells coupled by voltage-dependent gap junctions: the asymptotic dynamical limit. *Biosystems* 68: 213–222, 2003.
3. **Bukauskas FF, Bukauskiene A, Verselis VK.** Conductance and permeability of the residual state of connexin43 gap junction channels. *J Gen Physiol* 119: 171–185, 2002.
4. **Cousins HM, Edwards FR, Hickey H, Hill CE, Hirst GD.** Electrical coupling between the myenteric interstitial cells of Cajal and adjacent muscle layers in the guinea-pig gastric antrum. *J Physiol* 550: 829–844, 2003.
5. **Cuthbertson KS, Cobbold PH.** Phorbol ester and sperm activate mouse oocytes by inducing sustained oscillations in cell Ca²⁺. *Nature* 316: 541–542, 1985.
6. **De Roos AD, Willems PH, Peters PH, van Zoelen EJ, Theuvenet AP.** Synchronized calcium spiking resulting from spontaneous calcium action potentials in monolayers of NRK fibroblasts. *Cell Calcium* 22: 195–207, 1997.
7. **De Roos AD, Willems PH, van Zoelen EJ, Theuvenet AP.** Synchronized Ca²⁺ signaling mediated by intercellular propagation of Ca²⁺ action potentials in NRK fibroblasts. *Am J Physiol Cell Physiol* 273: C1900–C1907, 1997.
8. **Dupont G, Goldbeter A.** One-pool model for Ca²⁺ oscillations involving Ca²⁺ and inositol 1,4,5-trisphosphate as co-agonists for Ca²⁺ release. *Cell Calcium* 14: 311–322, 1993.
9. **Ernst U, Pawelzik K, Geisel T.** Delay-induced multistable synchronization of biological oscillators. *Phys Rev E* 57: 2150–2162, 1998.
10. **Falcke M.** Reading the patterns in living cells—the physics of Ca²⁺ signaling. *Adv Phys* 53: 255–440, 2004.
11. **Fogarty K, Kidd J, Tuft D, Thorn P.** Mechanisms underlying insp3-evoked global Ca²⁺ signals in mouse pancreatic acinar cells. *J Physiol* 526: 515–526, 2000.
12. **Freiesleben de Blasio B, Iversen J, Rottingen JA.** Intercellular calcium signalling in cultured renal epithelia: a theoretical study of synchronization mode and pacemaker activity. *Eur Biophys J* 33: 657–670, 2004.
13. **Harks EG, De Roos AD, Peters PH, de Haan LH, Brouwer A, Ypey DL, van Zoelen EJ, Theuvenet A.** Fenamates: a novel class of reversible gap junction blockers. *J Pharmacol Exp Ther* 298: 1033–1041, 2001.
14. **Harks EG, Torres JJ, Cornelisse LN, Ypey DL, Theuvenet AP.** Ionic basis for excitability in normal rat kidney (NRK) fibroblasts. *J Cell Physiol* 196: 493–503, 2003.
15. **Harks EG, Scheenen WJ, Peters PH, Zoelen EJ, Theuvenet AP.** Prostaglandin F_{2-α} induces unsynchronized intracellular calcium oscillations in monolayers of gap junctionally coupled NRK fibroblasts. *Pflügers Arch* 447: 78–86, 2003.
16. **Harks EG.** *Excitable Fibroblast! Ion Channels, Gap Junctions, Action Potentials and Calcium Oscillations in Normal Rat Kidney Fibroblasts* (PhD thesis). Nijmegen, The Netherlands: Radboud University Nijmegen, 2003.
17. **Henriquez CS, Plonsey R.** Effect of resistive discontinuities on wave-shape and velocity in a single cardiac fibre. *Med Biol Eng Comput* 25: 428–438, 1987.
18. **Henriquez AP, Vogel R, Muller-Borer BJ, Henriquez CS, Weingart R, Cascio WE.** Influence of dynamic gap junction resistance on impulse propagation in ventricular myocardium: a computer simulation study. *Biophys J* 81: 2112–2121, 2001.
19. **Höfer T, Politi A, Heinrich R.** Intercellular Ca²⁺ wave propagation through gap-junctional Ca²⁺ diffusion: a theoretical study. *Biophys J* 80: 75–87, 2001.
20. **Höfer T, Venance L, Giaume C.** Control and plasticity of intercellular calcium waves in astrocytes: a modeling approach. *J Neurosci* 22: 4850–4859, 2002.
21. **Imtiaz MS, Smith DW, van Helden DF.** A theoretical model of slow wave regulation using voltage-dependent synthesis of inositol 1,4,5-trisphosphate. *Biophys J* 83: 1877–1890, 2002.
22. **Imtiaz MS, Katnik CP, Smith DW, van Helden DF.** Role of voltage-dependent modulation of store Ca²⁺ release in synchronization of Ca²⁺ oscillations. *Biophys J* 90: 1–23, 2006.
23. **Joyner RW, Picone J, Veenstra R, Rawling D.** Propagation through electrically coupled cells. Effects of regional changes in membrane properties. *Circ Res* 53: 526–534, 1983.
24. **Joyner RW, Veenstra R, Rawling D, Chorro A.** Propagation through electrically coupled cells. Effects of a resistive barrier. *Biophys J* 45: 1017–1025, 1984.
25. **Joyner RW, van Capelle FJL.** Propagation through electrically coupled cells. *Biophys J* 50: 1157–1164, 1986.

26. Keener JP. The effects of discrete gap junction coupling on propagation in myocardium. *J Theor Biol* 148: 49–82, 1991.
27. Kusters JMAM, Dernison MM, van Meerwijk WPM, Ypey DL, Theuvenet APR, Gielen CCAM. Stabilizing role of calcium store-dependent plasma membrane calcium channels in action-potential firing and intracellular calcium oscillations. *Biophys J* 89: 3741–3756, 2005.
28. Kusters JMAM, Cortes JM, van Meerwijk WPM, Ypey DL, Theuvenet APR, Gielen CCAM. Hysteresis and bistability in a realistic cell model for calcium oscillations and action potential firing. *Phys Rev Lett* 98: 098107, 2007.
29. Lakatta E, Talo A, Capogrossi MC, Spurgeon H, Stern MD. Spontaneous sarcoplasmic reticulum Ca^{2+} release leads to heterogeneity of contractile and electrical properties of the heart. *Basic Res Cardiol* 87: 93–104, 1992.
30. Lin L, Crye M, Veenstra RD. Regulation of connexin43 gap junctional conductance by ventricular action potentials. *Circ Res* 93: 63–73, 2003.
31. Maltsev V, Vinogradova T, Lakatta E. The emergence of a general theory of the initiation and strength of the heartbeat. *J Pharmacol Sci* 100: 338–369, 2006.
32. Minneman KP. Alpha 1-adrenergic receptor subtypes, inositol phosphates, and sources of cell Ca^{2+} . *Pharmacol Rev* 40: 87–119, 1988.
33. Nathanson M, O'Sullivan PPA, Burgstahler A, Jamieson J. Mechanism of Ca^{2+} wave propagation in pancreatic acinar cells. *J Biol Chem* 267: 18118–18121, 1992.
34. Pikovsky A, Rosenblum M, Kurths J. *Synchronization: A Universal Concept in Nonlinear Sciences*. Cambridge: Cambridge University Press, 2003.
35. Politi A, Gaspers LD, Thomas AP, Hofer T. Models of IP_3 and Ca^{2+} oscillations: frequency encoding and identification of underlying feedbacks. *Biophys J* 90: 3120–3133, 2006.
36. Rohr S. Role of gap junctions in the propagation of the cardiac action potential. *Cardiovasc Res* 62: 309–322, 2004.
37. Sanders KM, Koh SD, Ward SM. Interstitial cells of Cajal as pacemakers in the gastrointestinal tract. *Annu Rev Physiol* 68: 307–343, 2006.
38. Sanderson MJ, Charles AC, Boitano S, Dirksen ER. Mechanisms and function of intercellular calcium signaling. *Mol Cell Endocrinol* 98: 173–187, 1994.
39. Savineau JP, Marthan R. Cytosolic calcium oscillations in smooth muscle cells. *News Physiol Sci* 15: 50–55, 2000.
40. Sneyd J, Wetton BTR, Charles AC, Sanderson M. Intercellular calcium waves mediated by diffusion of inositol triphosphate: a two-dimensional model. *Am J Physiol Cell Physiol* 268: C1537–C1545, 1995.
41. Tong D, Gittens JEI, Kidder GM, Bai D. Patch-clamp study reveals that the importance of connexin43-mediated gap junctional communication for ovarian folliculogenesis is strain specific in the mouse. *Am J Physiol Cell Physiol* 290: C290–C297, 2006.
42. Torres JJ, Cornelisse LN, Harks EGA, van Meerwijk WPM, Theuvenet APR, Ypey DL. Modeling action potential generation and propagation in NRK fibroblasts. *Am J Physiol Cell Physiol* 287: C851–C865, 2004.
43. Tsaneva-Atanasova KT, Yule D, Sneyd J. Calcium oscillations in a triplet of Pancreatic Acinar cells. *Biophys J* 88: 1535–1551, 2004.
44. Torihashi S, Fujimoto T, Trost C, Nakayama S. Calcium oscillation linked to pacemaking of interstitial cells of Cajal. *J Biol Chem* 277: 19191–19197, 2002.
45. Van Helden DF, Imtiaz MS. Ca^{2+} phase waves: a basis for cellular pacemaking and long-range synchronicity in the guinea pig gastric pylorus. *J Physiol* 548: 271–296, 2003.
46. Verheijck EE, Wilders R, Joyner RW, Golod DA, Kumar R, Jongasma HJ, Bouman LN, van Ginneken AC. Pacemaker synchronization of electrically coupled rabbit sinoatrial node cells. *J Gen Physiol* 111: 95–112, 1998.
47. Woods NM, Cuthbertson KS, Cobbold PH. Repetitive transient rises in cytoplasmic free calcium in hormone-stimulated hepatocytes. *Nature* 319: 600–602, 1986.
48. Yao Y, Parker I. Ca^{2+} influx modulation of temporal and spatial patterns of inositol triphosphate-mediated Ca^{2+} liberations in *Xenopus* oocytes. *J Physiol* 476: 17–28, 1994.
49. Ypey DL, van Meerwijk WPM, DeHaan RL. *Synchronization of Cardiac Pacemaker Cells by Electrical Coupling*. The Hague: Nijhoff, 1982.
50. Zhao J, Imtiaz M, van Helden D. Ca^{2+} oscillations and pacemaker potentials underlying vasomotion in guinea-pig lymphatic smooth muscle. *Proc Aust Health Med Res Congr 1st Melbourne*, 2002, abstr. 1148.